

Properties of Capped Nanotubes When Used as SPM Tips

J. A. Harrison* and S. J. Stuart

Chemistry Department, U.S. Naval Academy, Annapolis, Maryland 21402

D. H. Robertson

Department of Chemistry, IUPUI University, Indianapolis, Indiana 46202-3274

C. T. White

Department of Materials, University of Oxford, Parks Road, Oxford OX11 3PH, U.K.

Received: July 11, 1997; In Final Form: September 23, 1997[®]

The utility of hemispherically capped single-wall carbon nanotubes for use as scanning force microscope tips is investigated for the first time using molecular dynamics. These simulations show that [10,10] armchair nanotubes recover reversibly after interaction with a hydrogen-terminated diamond (111) substrate. The [10,10] tube exhibits two mechanisms for releasing stresses induced by indentation: a marked inversion of the capped end, from concave to convex, and finning along the tube's axis.

Smalley and co-workers recently proposed that carbon nanotubes might constitute well-defined tips for scanning probe microscopy (SPM).¹ In that work, individual multiwalled nanotubes several micrometers in length were attached to the silicon cantilevers of conventional scanning force microscopes. The slenderness of the tips permitted imaging of 400 nm-wide and 800 nm-deep trenches etched in TiN-coated aluminum on a silicon wafer. While a conventional pyramidal tip was too wide to reach the bottom of such a trench, the nanotube was able to image the roughness of the surface at the bottom of the trench.

Multiwalled nanotubes were shown to perform well as SPM tips when used in tapping mode, due to their desirable combination of stiffness and flexibility. The stiff nature of the nanotubes along their axial dimension ensures that a considerable force (called the Euler buckling force) is needed to induce bending when a tube encounters the surface at near-normal incidence.^{1,2} Yet the flexibility of the tubes in transverse directions allows them to bend easily, with little additional force, once the Euler buckling force is exceeded.

The large Young's modulus of carbon nanotubes (approximately the same as the in-plane modulus of graphite or higher^{2–5}) should allow them to be used over a wide range of applied forces, with the Euler buckling force providing an upper limit for the longer tubes (length > 10 nm²) that could be used to prevent damage to the substrate. Since the value of the Euler buckling force can be varied by adjusting the tip's length, the mechanical properties of the tip can be tuned. On the basis of these observations, Smalley and co-workers speculated that single-walled nanotubes, such as a [10,10] nanotube, with or without chemical derivatization at specific sites on the tip, might provide ultimate nanoprobe.¹

With this in mind, and given the fact that single-walled nanotubes (SWNT) can now be prepared experimentally,⁶ we have used molecular dynamics (MD) simulations to examine the use of capped SWNT as SPM tips. In particular, we have used the [10,10] nanotube thought to be preferentially produced to indent a hydrogen-terminated diamond (111) surface. This

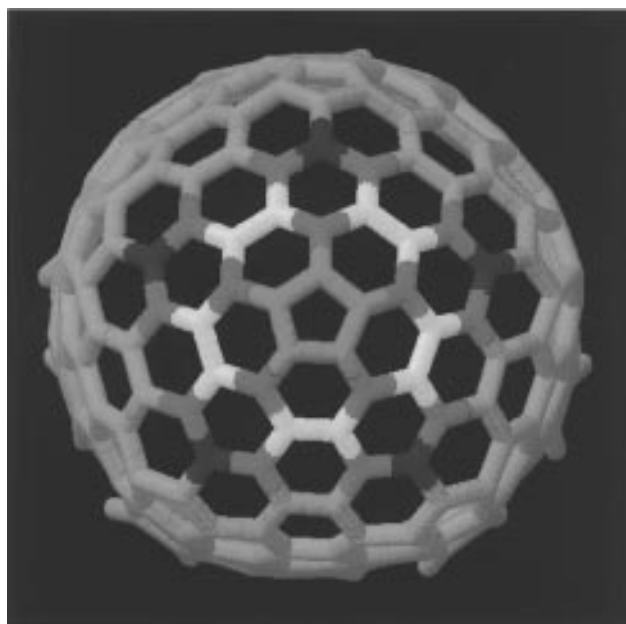


Figure 1. Snapshot of the cap of the [10,10] nanotube. The red spheres represent the atoms that compose the pentagon at the vertex of the cap. The red, cyan, and yellow cap atoms are the first to be inverted during the indentation (point B in Figure 3). The green and the blue atoms are "pushed" inside the tube as part of the second inversion event (point C in Figure 3). Magenta atoms do not invert during the indentation. Tube atoms that are not part of the hemispherical caps are colored gray.

[10,10] nanotube was capped with a C_{5v} hemifullerene dome having a single pentagon centered on a 5-fold symmetry axis at the vertex (Figure 1). The nanotube contained 850 carbon atoms and was approximately 53 Å long from base to cap. The carbon atoms on the open end of the tube were terminated with hydrogens to satisfy the valence requirements of carbon. The diamond surface contained 5120 sp^3 -hybridized carbon atoms and 512 hydrogen atoms that were used to terminate the two free surfaces of the diamond lattice.

The forces governing the motion of the atoms were described using the latest version of the reactive empirical bond-order (REBO) potential developed by Brenner,^{7,8} based on a formalism

* To whom correspondence should be addressed.

[®] Abstract published in *Advance ACS Abstracts*, November 1, 1997.

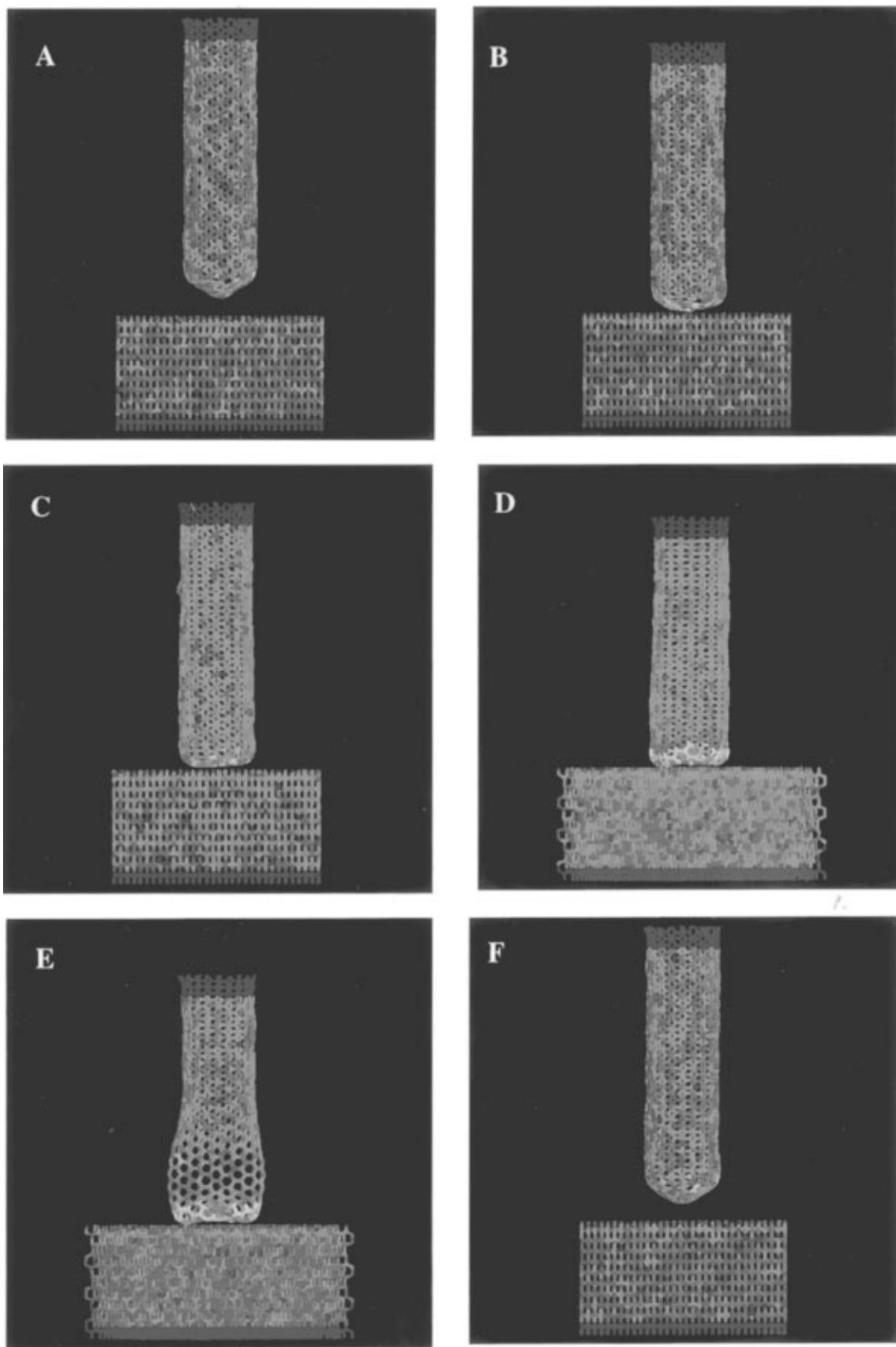


Figure 2. Snapshots from the MD simulations of the interaction of a capped [10,10] nanotube with a hydrogen-terminated diamond (111) surface. The simulation times are 0.0, 50.0, 55.0, 83.0, 89.0, and 200.0 ps in (A), (B), (C), (D), (E), and (F), respectively. The colors blue, green, yellow, and red correspond to increasing values of the von Mises stress.

proposed by Tersoff.⁹ This potential and its antecedents⁸ have been used successfully to study problems ranging from the initial stages of diamond growth¹⁰ to the mechanical properties of isolated carbon nanotubes.^{2,11} The equations of motion were

integrated using the velocity Verlet algorithm¹² with a time step of 0.25 fs. The uppermost four layers of the nanotube and the lowest three layers of the diamond surface were held rigid throughout the course of the simulations (Figure 2A). Two

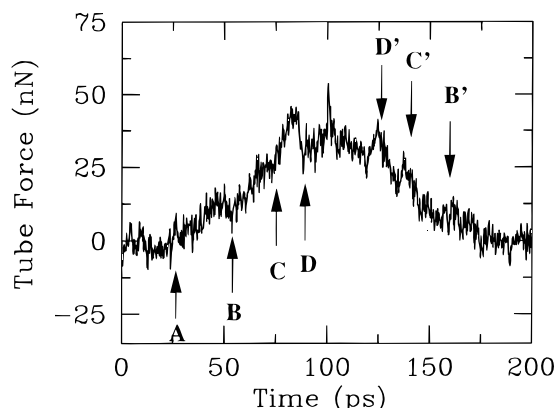


Figure 3. Normal force on the rigid layers of the [10,10] nanotube as a function of time. Data points are averaged over 200 fs intervals. The nanotube makes contact with the surface at point A. The significance of points B (B'), C (C'), and D (D') are described in the text.

distinct thermostats¹³ were applied to atoms in the middle of the tube and the substrate to maintain the temperature at 300 K, although most of the atoms in the simulation acted under no constraints whatsoever. Indentation (or retraction) was performed by moving the rigid layers of the tube at a constant velocity of 10 m/s toward (or away from) the diamond substrate. Limits on computation time constrain this indentation velocity to be many orders of magnitude larger than the 10^{-8} m/s speeds typically used in nanoindentation experiments,¹⁴ and still several orders of magnitude greater than the 10^{-1} m/s speeds commonly used in tapping mode. Even at 10 m/s, however, the tube was observed to behave reversibly with adequate time for thermal and structural equilibration as the indentation proceeded. We conclude that the simulation accurately describes the behavior that would be observed under much slower loading rates.

The force on the rigid tube atoms of the [10,10] tube as a function of the simulation time is shown in Figure 3. This force trace shows that there are distinct regions where the force rises linearly as the tube is pushed toward the surface, separated by

relatively sharp discontinuities. The slope of this trace in the linear regions is related to the response of the nanotube,¹⁵ and the discontinuities mark distinct changes in the tube's conformation. Three of these conformational changes occur during indentation, and another three occur during extraction. These points are marked by the labels B, C, and D in Figure 3. (Point A represents the first contact between the nanotube and the surface and does not represent a conformational change.) Each of these events is accompanied by a change in slope in the force trace, demonstrating that the mechanical properties of the tube vary with geometry.

The first such change occurs at point B in Figure 3. Examination of the detailed atomic trajectories indicates that the 20 atoms on the end of the cap inverted at this point, "popping" approximately 1.0 \AA into the interior of the tube in less than 50 fs (see Figure 4). After this concerted change from a convex cap geometry to a concave one, the pentagon and five hexagons at the extreme end of the nanotube had retracted so that they were further from the surface than the neighboring atoms. (Cf. Figure 1, in which the inverted cap atoms are colored red, cyan, and yellow.)

The cap inversion occurred when the tube had been compressed by approximately 2.5 \AA , to a total length of 50.5 \AA . The decrease in force in Figure 3 associated with the cap inversion indicates that this is a mechanism for releasing pent-up stresses on the nanotube's cap. This observation is confirmed by parts B and C of Figure 2, snapshots of the simulation in which atoms are colored coded according to the local value of the von Mises shear (stress). Prior to the cap inversion, compressive stresses (red atoms) are clearly visible at the vertex of the tube (Figure 2B). These stresses are reduced after cap inversion (Figure 2C). The rapid nature of the inversion and the amount of movement are evident when average tip atom positions are plotted as a function of time (Figure 4).

The slope in the force trace (Figure 3) displays a second discontinuity at point C. At this point, when the tube had been compressed by 3.5 \AA , the built-up stresses were released by

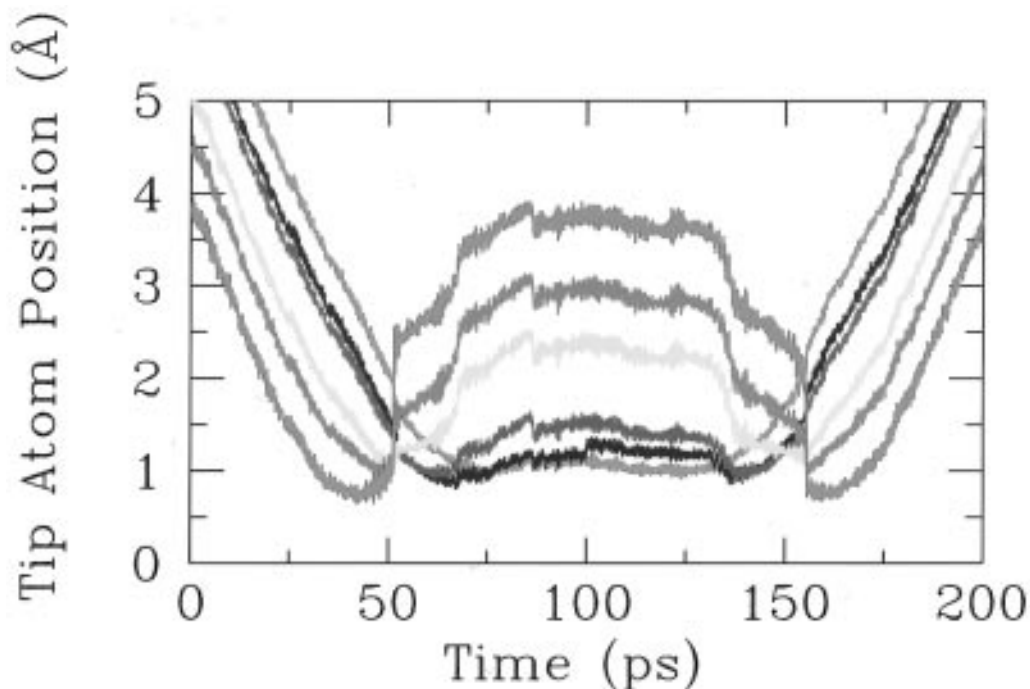


Figure 4. Average Z position of the [10,10] tube cap atoms as a function of simulation time. Results for the indentation and the pullback are shown with colors corresponding to those used in Figure 1. For example, the red line represents the average Z position of all the atoms from the pentagon of the hemispherical cap, colored red in Figure 1.

the inversion of the next ring of five hexagons in the tube's cap (atoms colored green and blue in Figure 1). These atoms joined the atoms already inside the tube and remained further from the surface than the remaining cap atoms (atoms colored magenta in Figure 1) for the remainder of the indentation (Figure 4).

Further inversion events were not observed under continued indentation. Instead, additional stresses on the tip were released through the process of "finning" that has been observed in previous MD simulations of uncapped nanotubes.^{2,3} In this mechanism of relaxation, two opposing walls of the nanotube collapse inward, giving the tube an elliptical (or even dumbbell-shaped) cross section in one region. In this conformation, the stresses are concentrated near the cap in the thin region of the nanotube (see Figure 2E). The finning event occurs at the point marked D on the force trace (Figure 3). As in previous studies,² formation of an initial fin was later followed by the formation of a second fin at right angles to the first, although this event is not shown in Figure 3.

When the tube was withdrawn from the surface at the same constant velocity, the conformational changes were observed to be completely reversible. Each of the relaxation events observed under indentation has a corresponding feature in the retraction portion of the curve (see Figure 3). In the events labeled D', C', and B' in Figure 3, the finned region of the tube is restored to a circular cross section, then the cap atoms in the second row of hexagons emerge from the inverted region of the tube, and finally the vertex atoms "pop" back out to restore the hemispherical cap. After complete retraction of the simulated SPM tip, the nanotube was found to be in the same conformation as when the simulation was started, with no damage (Figure 2F).

The conformational changes observed in these simulations indicate that a single tube can have several different responses as it undergoes different modes of compression during indentation. These results are important in light of the considerable interest in the Young's modulus of carbon nanotubes.²⁻⁴ The modulus that corresponds to compression of only the tubular portion of the nanotube (i.e., excluding the tip) can be obtained from the simulation data after the second cap inversion and before the formation of the first fin (between points C and D on Figure 3). Using the method outlined by Pharr et al.,¹⁶ a tube radius of 6.91 Å, and Poisson ratio of the tube of $\nu = 0.19$,² a Young's modulus of approximately 910 GPa is obtained for the capless portion of the nanotube.¹⁷ This value of Young's modulus falls within the range of reported values, both experimental and theoretical, for other nanotubes.²⁻⁶

It is important to realize that the initial modes of compression as the tip encounters the surface are much softer than the tubular compression discussed above and could lead to an underestimation of the Young's modulus for the tube by experiment. At loads of 20 nN and lower, the primary mechanism of tip deformation is a flattening of the tube's cap prior to the cap inversion. If the simulation data in this regime were to be used to estimate Young's modulus using the technique of Pharr et al.,¹⁶ a value of only 85 GPa would result. Similarly, between points B and C in Figure 3, the tube's cap continues to be deformed prior to the second inversion event. If data from that region were used, a Young's modulus of approximately 520 GPa would result.

It should be noted that the 53-Å tube simulated here is considerably shorter than the 250 nm tubes used in experiment.¹ Consequently, there are certain motions of the tube that will be diminished (or absent), compared to experiment. These include the thermal vibrations of the tip,⁵ which increase in magnitude

with tube length, and the Euler buckling failure mode, which is expected to be observed only in tubes of greater than 10 nm in length.² The cap inversion and finning modes, on the other hand, should be fully representative of deformations in larger tubes.

These simulations demonstrate that capped nanotubes, although undergoing complex deformations, have the remarkable ability to recover reversibly when pushed into a hard substrate, such as diamond, with forces of up to 43 nN. This property, in addition to the convenient size and stiffness of nanotubes, makes them outstanding candidates for SPM tips.¹ Yet for large-radius tubes, the complex inversion and finning mechanisms demonstrated in the current study indicate that the simple approximations frequently used in approximating tip stiffness are not valid over the entire experimentally achievable load range. Our results indicate that carbon nanotubes with sufficiently large diameters can have a range of different responses, depending on the applied normal force. Simulations such as those described here should continue to provide valuable input to experimental studies, by providing the physical parameters needed to make nanotubes useful probes of atomic-level surface structure.

Acknowledgment. The authors thank D. W. Brenner, B. I. Dunlap, and J. W. Mintmire for helpful discussions. C.T.W. also thanks the Department of Materials and especially D. G. Pettifor for hospitality during his sabbatical stay at Oxford. This work was supported by the U.S. Office of Naval Research (ONR) under contracts N00014-97-WX-20019 and N00014-97-WX-20238 and the Materials Modeling Laboratory at Oxford.

References and Notes

- (1) Dai, H.; Hafner, J. H.; Rinzler, A. G.; Colbert, D. T.; Smalley, R. E. *Nature* **1996**, *384*, 147.
- (2) Yakobson, B. I.; Brabec, C. J.; Bernholc, J. *Phys. Rev. Lett.* **1996**, *76*, 2511.
- (3) Cornwell, C. F.; Wille, L. T. *Solid State Commun.* **1997**, *101*, 555.
- (4) Ruoff, R. S.; Lorents, D. C. *Carbon* **1995**, *33*, 925. Tersoff, J.; Ruoff, R. S. *Phys. Rev. Lett.* **1994**, *73*, 676.
- (5) Treacy, M. M. J.; Ebbesen, T. W.; Gibson, J. M. *Nature* **1996**, *381*, 678.
- (6) Iijima, S.; Ichihashi, T. *Nature* **1993**, *363*, 603. Bethune, D. S.; Kiang, C. H.; de Vries, M. S.; Gorman, G.; Savoy, R.; Vazquez, J.; Beyers, R. *Nature* **1993**, *363*, 605. Thess, A.; Lee, R.; Nikolaev, P.; Dai, H.; Petit, P.; Robert, J.; Xu, C.; Lee, Y. H.; Kim, S. G.; Rinzler, A. G.; Colbert, D. T.; Scuseria, G. E.; Tománek, D.; Fischer, J. E.; Smalley, R. E. *Science* **1996**, *273*, 483.
- (7) This potential energy function was recently reparametrized to accurately reproduce the elastic constants of diamond and graphite while maintaining all of its original properties (Brenner, D. W.; Sinnott, S. B.; Shenderova, O. A.; Harrison, J. A., unpublished).
- (8) Brenner, D. W. *Phys. Rev. B* **1990**, *42*, 9458. Brenner, D. W.; Harrison, J. A.; White, C. T.; Colton, R. J. *Thin Solid Films* **1991**, *206*, 220.
- (9) Tersoff, J. *Phys. Rev. Lett.* **1986**, *56*, 632. *Phys. Rev. B* **1988**, *37*, 6991.
- (10) Garrison, B. J.; Dawnkaski, E. J.; Srivastava, D.; Brenner, D. W. *Science* **1992**, *255*, 835.
- (11) Robertson, D. H.; Brenner, D. W.; Mintmire, J. W. *Phys. Rev. B* **1992**, *45*, 12592.
- (12) Swope, W. C.; Andersen, H. C.; Berens, P. H.; Wilson, K. R. *J. Chem. Phys.* **1982**, *76*, 637.
- (13) Adelman, S. A.; Doll, J. D. *J. Chem. Phys.* **1976**, *64*, 2375. Adelman, S. A. *Adv. Chem. Phys.* **1980**, *44*, 143.
- (14) Bhushan, B., Ed. *Handbook of Micro/Nanotribology*, 1st ed.; CRC Press: Boca Raton, FL, 1995; pp 30, 343.
- (15) More precisely, the Young's modulus is obtained from the variation of the normal force with penetration depth.¹⁶
- (16) Pharr, G. M.; Oliver, W. C.; Brotzen, F. R. *J. Mater. Res.* **1992**, *7*, 613.
- (17) Strictly speaking, the method outlined in ref 16 requires calculation of the contact stiffness during the initial stages of tip retraction. Because the indentations discussed here are largely elastic, the contact stiffness can be obtained equally well from the indentation data.